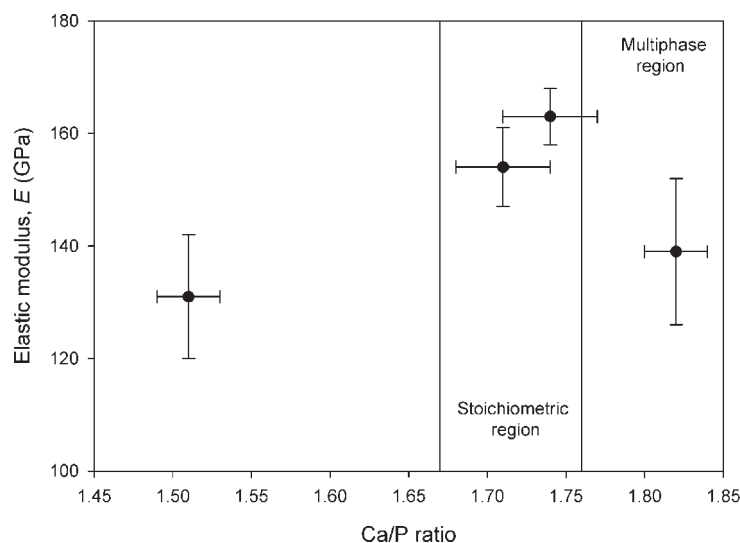# Influence of the Chemical Composition on the Phase Constitution and the Elastic Properties of RF-Sputtered Hydroxyapatite Coatings

Rony Snyders,* Etienne Bousser, Denis Music, Jens Jensen, Stéphane Hocquet, Jochen M. Schneider

We have studied the influence of chemical composition on the constitution and elastic properties of dense radio-frequency (RF)-sputtered hydroxyapatite (HA) coatings. The chemical composition was modified by varying the RF sputtering power density ($P_D$). As the $P_D$ was increased by 240%, the Ca/P ratio measured by X-ray photoelectron spectroscopy increased from ≈1.51 to ≈1.82. X-ray diffraction indicates phase pure hexagonal HA except for the sample prepared at the highest $P_D$ where CaO and $Ca_3(PO_4)_2$ also form. Deviations from the stoichiometric Ca/P ratio result in reduction of the elastic modulus. For Ca/P = $1.51 \pm 0.02$, the elastic modulus decreases by ≈15%. This may be due to incorporation of Ca vacancies in the lattice, while for Ca/P = $1.82 \pm 0.02$, the average elastic modulus decreases by ≈10% due to formation of additional phases.

R. Snyders, D. Music, J. M. Schneider
Materials Chemistry, RWTH Aachen University, 52056 Aachen, Germany
Fax: +003265373841; E-mail: rony.snyders@umh.ac.be
R. Snyders
Current Address: LCIA, Université de Mons, 1, avenue Copernic, 7000 Mons, Belgium
E. Bousser
Department of Engineering Physics, Ecole Polytechnique de Montréal, Montreal, Qc, Canada H3C 3A7
J. Jensen
Division of Ion Physics, Uppsala University, Box 534, 75121 Uppsala, Sweden
S. Hocquet
Belgian Ceramic Research Center, Avenue Gouverneur Cornez, 4, 7000 Mons, Belgium

## Introduction

Calcium phosphates are suitable materials for biomedical applications.[1] Especially in the case of hydroxyapatite, $Ca_5(PO_4)_3OH$ (space group P6₃/m, hereafter HA), a lot of attention has been drawn due to the fact that it mimics the mineral component of natural bone.[1] Major drawbacks of HA are associated with the inadequate mechanical properties of the bulk material. HA possesses a low fatigue resistance and is brittle, inhibiting its usage as implant in load-bearing applications.[2,3] Therefore, HA coatings are usually deposited on a load-bearing implant, mainly Ti and its alloys, in order to fulfill requirements for loaded applications, such as total joint replacement and dental root implant, by combining the mechanical

WILEY InterScience®
DISCOVER SOMETHING GREAT

Influence of the Chemical Composition on the Phase Constitution and the Elastic Properties . . .

Plasma Processes
and Polymers

strength of the bulk material and the biocompatibility of the HA coating.[4] Since the first tests in 1985,[5] it has been reported that HA coatings significantly enhance clinical success of implants. Indeed, it has been suggested that, with long implantation time, synthetic HA coatings can be replaced by bone owing to a cellular degradation process of HA coatings caused by osteoclastic activity.[6] This phenomenon enables a bone remodeling response similar to any other parts of the skeleton.

The most common commercial method to produce HA coatings on metallic implant substrates is plasma spraying which allows for high deposition rates.[7] However, several significant disadvantages are reported for this technique such as poor adhesion of coatings on metallic substrates,[8–13] alterations in HA structure and composition,[12,13] poor thickness uniformity,[12] and significant porosity.[9–11] Consequently, new deposition processes have been investigated including thermal spraying,[14] pulsed laser deposition (PLD),[9,11,15] sol–gel,[16] and radio-frequency (RF) magnetron sputtering.[11–13,17]

RF magnetron sputtering of HA has been investigated for the last 15 years. The main advantages of this process are the formation of adherent, uniform, and dense HA coatings.[11–13,17–19] However, one of the drawbacks of this technique is the formation of amorphous or, by using higher sputtering power, only weakly crystalline HA coatings. RF-sputtered coatings with high crystal quality can be obtained by post-deposition treatment, such as annealing,[11–13] hydrothermal treatment,[20] or laser irradiation.[21]

The main limitation of RF sputtering of HA is the possible alteration of the HA structure and composition.[11–13,18,19] Actually, the Ca/P ratios measured for RF-sputtered HA films are often higher than the stoichiometric ratio of 1.67.[22] This has been reported to result in the incorporation of Ca or CaO particles in the sputtered films.[23] Other Ca-P-based crystalline phases such as tricalcium phosphate, $Ca_3(PO_4)_2$ (TCP),[10,13] dicalciumphosphate, $CaHPO_4$ (DCP),[9] calcium pyrophosphate, $Ca_2P_2O_7$ (SYN),[13] or tetracalcium phosphate, $Ca_4P_2O_9$ (TTCP),[12] have also been detected in HA films.

It has been demonstrated that the presence of CaO in HA coatings reduces dramatically their biocompatibility since CaO causes severe cytotoxicity and may therefore lead to inflammation of the surrounding tissue.[24] On the other hand, the other Ca-P-based phases, namely DCP, TCP, TTCP, or SYN, present biocompatibility level comparable to the one of HA but with lower osteoconductivity.[13] Phase purity and stoichiometry of HA coatings can be tailored with process parameters such as sputtering power,[12,13] pressure,[13] sputtering gas composition,[25] or substrate bias.[26]

Despite their importance, only few authors have focused their attention on the mechanical properties of RF-deposited HA coatings. Recently, we reported the elastic properties of pure and dense HA deposited by RF sputtering measured by nanoindentation and compared the results with our *ab initio* values. The results suggest an experimental elastic modulus ($E$) of $147 \pm 10$ GPa which deviates about 10% from the calculated one (132 GPa).[17] Nevertheless, to the best of our knowledge, no systematic reports on the relationship between synthesis conditions, film composition and constitution, as well as elastic properties of HA-sputtered films are available. Therefore, the aim of this work is to evaluate the influence of the composition on the constitution and elastic properties of HA coatings. The experimental methodology employed to reach this goal was to systematically modify the film composition by varying the cathode power density.

We have found that the elastic modulus of HA exhibits the maximum value close to the stoichiometric Ca/P ratio. This value is consistent with previously reported *ab initio* data.[17]

## Methodology

Pure HA powder (total content of heavy metal <50 ppm) was prepared by hydrothermal synthesis from calcium and phosphorus salts. As the grain size of the powder was too small to be compacted (1.70 μm), polyethylene glycol (PEG; molecular weight of 2 kDa, Sigma–Aldrich), was added as binder. PEG with a concentration of 2 wt.-% was dissolved in ethanol and the resulting solution was mixed with the HA powder. After ethanol evaporation, the mixture was slowly compacted in a hydraulic laboratory press at a pressure of 75 MPa and then relaxed, following several decompression plateaus to allow the compacted HA sample to eliminate stress. The sample was then fired at 1 300 °C for 24 h in a furnace in air in order to consolidate its structure. After cooling, the sample was cut in a cylindrical shape with a 90 mm diameter and a 5 mm thickness.

HA coatings were deposited on electrically grounded silicon wafers by RF sputtering in a turbomolecularly pumped chamber with a base pressure of approximately $4 \times 10^{-4}$ Pa ($3 \times 10^{-6}$ Torr). Depositions were performed in a pure Ar atmosphere at a pressure of 0.65 Pa (5 mTorr). The RF power density ($P_D$) was determined by dividing the measured RF power applied to the sintered HA target by the total target area and was studied in the range of 1.0–2.4 W · cm$^{-2}$. The target to substrate distance was 8 cm. The resulting coating thickness was determined by profilometry. With the aim to crystallize HA coatings, they were annealed for 1 h at 550 °C in air, according to the procedure proposed by Nelea et al.[10] Table 1 contains the deposition parameters of HA samples as well as their thickness and deposition rate.

*Table 1.* Experimental conditions during hydroxyapatite depositions: RF power density, deposition rate, working pressure, and film thickness.

| RF power density | Deposition rate | Working pressure | Thickness |
|---|---|---|---|
| $W \cdot cm^{-2}$ | $nm \cdot min^{-1}$ | Pa | μm |
| 1.0 | 0.7 | 0.65 | $2.06 \pm 0.10$ |
| 1.5 | 0.9 | 0.65 | $0.88 \pm 0.10$ |
| 2.0 | 2.5 | 0.65 | $0.74 \pm 0.04$ |
| 2.4 | 3.0 | 0.65 | $1.41 \pm 0.07$ |

Structural characterization was performed in a D8 Discover General Area Detection Diffraction System with HI-STAR 1 024 × 1 024 pixels 2D detector (Bruker-AXS Inc.). Cu $K_\alpha$ radiation was used. The generator was operated with an acceleration voltage and current of 40 kV and 40 mA, respectively. The detector to sample distance was 15 cm. The goniometer was equipped with a pinhole collimator, a laser, and a camera for focusing on the area of the sample to be measured. The incidence angle was 5° with a frame width of 32° and a measurement time of 240 s per frame was employed.

The films density has been evaluated by combining time-of-flight energy-elastic recoil detection analysis (Tof-EERDA)[27,28] using 40 MeV iodine ions and films thickness measurements. X-ray photoelectron spectroscopy (XPS) was used to measure the chemical composition of the HA coatings. High-resolution spectra in the Ca2p and P2p regions were recorded to obtain the Ca/P ratio. This ratio was derived from peak areas using photoionization cross-sections calculated by Wagner et al.[29]

Hardness ($H$) and reduced elastic modulus ($E_r$) values were determined by nanoindentation using a Hysitron TriboIndenter instrument equipped with a Berkovich tip. The data were processed using the Hysitron software providing load–displacement curves corrected for thermal drift and machine constants (frame compliance, transducer spring force, and electrostatic force constants). Load–displacement curves were analyzed according to the Oliver–Pharr method.[30] For each sample, $H$ and $E_r$ were obtained from 100 indentations with applied loads from 100 to 10 000 μN while the penetration depth ranged between 7 and 230 nm depending on the sample thickness. Nanoindentation curves with discontinuities due to crack formation have not been considered. The Hysitron TriboIndenter instrument was calibrated by nanoindenting in a fused silica standard and fitting the area function with a known reduced elastic modulus of 69.6 GPa. It is widely accepted that, in order to render substrate effects negligible, penetration depths should not exceed 10% of the total coating thickness.[31] Therefore, the obtained $H$ and $E_r$ values are measured at nanoindentation depths between ≈35 and ≈50 nm. Finally, the elastic modulus was calculated based on a Poisson's ratio of 0.28 determined by ultrasonic method by Grenoble et al.[32]

Elastic properties of HA coatings were estimated using *ab initio* calculations. Density functional theory[33] was used within the Vienna *ab initio* simulation package (VASP), where ultrasoft pseudopotentials are employed.[34,35] The generalized gradient approximation was applied in all calculations. The integration in the Brillouin zone is done on special $k$ points determined according to Monkhorst-Pack. Reduced unit cells containing 22 atoms, i.e., one formula unit, were studied on a mesh of 5 × 5 × 5 irreducible $k$ points. Two configurations were probed: $Ca_5(PO_4)_3OH$ and $Ca_4(PO_4)_3OH$ (1 Ca vacancy per formula unit). The convergence criterion for the total energy was 0.01 meV within a 495 eV cutoff. Atomic positions and internal free parameters were relaxed. Full structural relaxation was carried out at every volume.[36] The energy–volume curves obtained were used to calculate bulk modulus by fitting them to the modified Morse functions.[37] Elastic moduli were estimated from the bulk modulus data using previously obtained Poisson's ratio.[17]

## Results and Discussion

Table 1 contains the RF power density applied to the HA target ($P_D$), the deposition pressure ($p_T$), the corresponding deposition rate ($R_D$), and the thickness of the deposited coating. $R_D$ values range between 0.7 and 3.0 $nm \cdot min^{-1}$. These values are relatively low when compared to other published data.[12,25] As an example, van Dijk et al. reported $R_D$ of about 5 $nm \cdot min^{-1}$ for 200 W RF power applied to the HA target.[12] Nevertheless, in another work, the same authors have reported a significant decrease in $R_D$ when even small amount of $O_2$ is present in the discharge.[25] Actually, they have demonstrated that even 1% $O_2$ in the sputtering gas mixture reduces the sputtering yield of HA by 60%.[25] The low $R_D$ value measured during our experiment could therefore be explained by the presence of residual $O_2$ or $H_2O$.

Influence of the Chemical Composition on the Phase Constitution and the Elastic Properties . . .

Plasma Processes
and Polymers

Figure 1 shows the evolution of the Ca/P ratio and of the density of the films as a function of $P_D$. The Ca/P ratio increases from $1.51 \pm 0.02$ to $1.82 \pm 0.02$ as the $P_D$ is increased, with a close to stoichiometric ratio of $1.71 \pm 0.03$ for $P_D = 1.5$ W·cm$^{-2}$. This dependence of the Ca/P ratio on the $P_D$ has already been reported by van Dijk et al.[12] Nevertheless, based on statistical analysis of the data, the authors reported only a weak correlation between sputtering power and films composition. The Ca/P ratio values measured for our films range from 1.51 to 1.82 and hence include the stoichiometric value of 1.67. For most of the RF-sputtered HA films, a Ca/P ratio larger than 1.67 is reported.[12,13,18] The Ca excess is attributed to numerous mechanisms such as Ca[12] or CaO[9,12] incorporation in the growing films, preferential resputtering of P from the growing film, and more efficient scattering of P atoms compared to Ca atoms by the residual gas and Ar.[12] It has been reported that the discharge power, working pressure, sputtering gas composition, substrate bias, and annealing conditions influence strongly the Ca/P ratio.[12,13,23,25,26] The Ca/P ratio of RF-sputtered HA coatings decreases to close to the stoichiometric value when working pressure[13] and discharge power[12] are decreased and when the annealing temperature is increased.[23] In the latter case, the Ca/P ratio decrease is accompanied by appearance of undesired phases such as CaO and TCP.

On the other hand, it has also been demonstrated that incorporation of a small quantity of $O_2$ in the discharge leads also to a decrease in the Ca/P ratio.[25] The comparatively low Ca/P ratio values measured in the present work can be related to the relatively low working pressure and power density used and to the presence of residual oxygen-containing gas in the chamber: With 5% $O_2$ in the gas mixture and for similar experimental parameters ($P_D = 0.8$ W·cm$^{-2}$, $p_T = 0.39$ Pa (3 mTorr), and $R_D = 1.5$ nm·min$^{-1}$) to the ones used in the present work ($P_D = 1.0$–2.4 W·cm$^{-2}$, $p_T = 0.65$ Pa (5 mTorr), and $R_D = 0.7$–3 nm·min$^{-1}$), Nelea et al. have measured Ca/P ratios of about 1.73–1.78.[10] Since the deposition rate and Ca/P ratio values reported by Nelea et al. are comparable to the data presented here, it is reasonable to assume that this is due to the presence of residual oxygen-containing gas during sputtering. This is consistent with the $R_D$ data analysis. Additionally, it is known that materials with a large affinity to residual gas form reaction products on the cathode surface[38] as well as during alumina,[39] strontium titanate,[40] and boron suboxide[41] growth.

XRD diffractograms of HA coatings after annealing procedure are presented in Figure 2 together with the one of the HA target. Contrary to the one of the target, diffractograms of annealed films present a strong (000l) preferential orientation (with the c-axis perpendicular to the substrate surface) characteristic of HA films deposited by RF magnetron sputtering.[12] The diffractogram of the target as well as the ones of samples with Ca/P ratio values $\leq 1.74 \pm 0.03$ are consistent with the diffraction lines of hexagonal HA, h-HA (JCPDS card No. 9-0432). The diffractogram of the sample with a Ca/P ratio value of $1.82 \pm 0.02$ differs from all other samples due to the appearance of diffraction lines at 21.96°, 28.94°, 33.02°, 37.24°, and 39.82°. Except for the one at 37.24°, most of the diffraction lines could also be attributed to h-HA. Nevertheless, other possible Ca-P-based phases such as β-TCP (JCPDS card No. 9-169) and CaO (JCPDS card No. 37-1497) could also match with these new lines. Both of these phases have already been observed in RF-sputtered HA films.[10,13] Unfortunately, due to the presence of h-HA, CaO, and TCP diffraction lines in similar 2θ regions, it is not straightforward to deduce the phase composition of this sample only from the corresponding diffractogram.

The formation of CaO, may be due to partial decomposition of HA during the sputtering process, results in an increase in the Ca/P ratio of the films, while formation of TCP results in a decrease in the Ca/P ratio since the stoichiometric Ca/P ratio for this phase is 1.50. XPS data show an increase in the
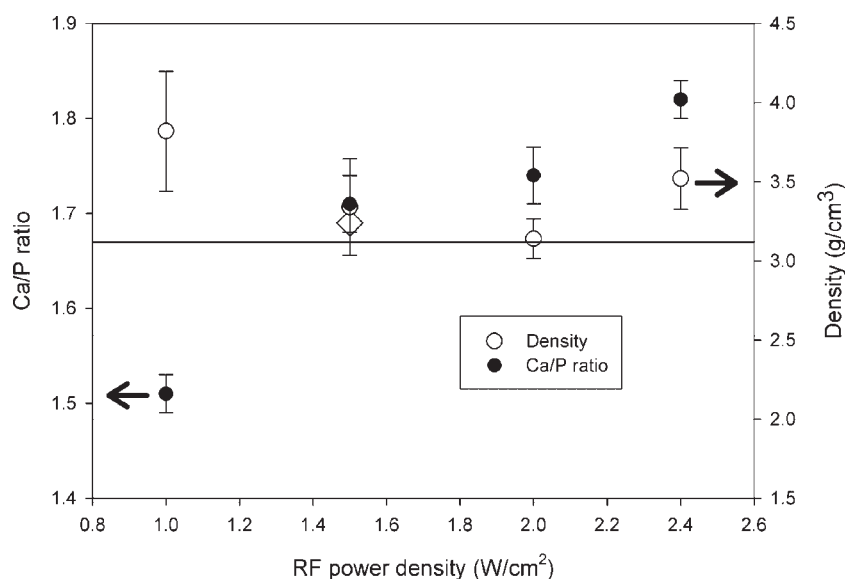


Figure 1. Density and Ca/P ratio as a function of the RF power density applied to the HA target. The unfilled diamond symbol corresponds to previously published data for pure, dense, and stoichiometric HA.[17] The horizontal line indicates the stoichiometric HA Ca/P ratio of 1.67[18] and the stoichiometric HA density of 3.15 g·cm$^{-3}$.[22]
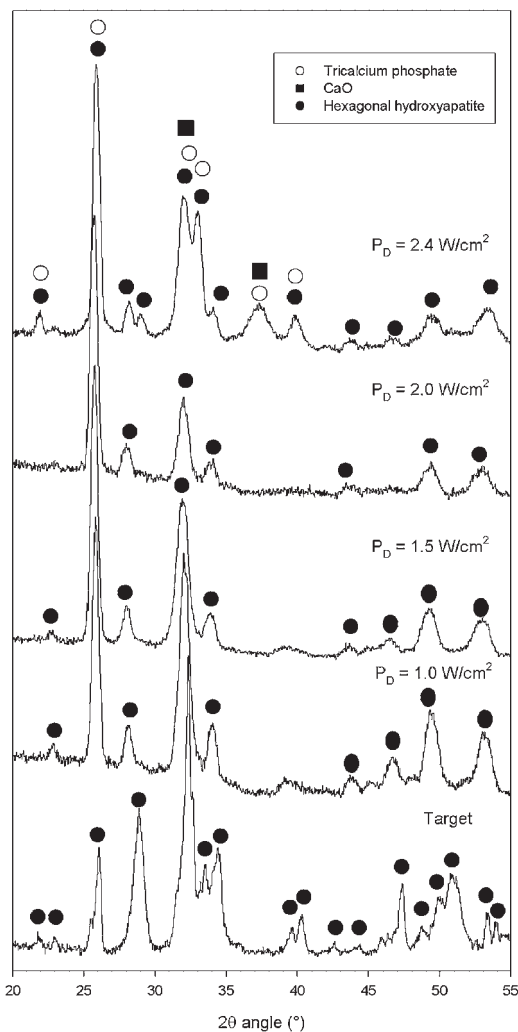
*Figure 2.* HA target diffraction pattern and evolution of the diffraction pattern of the films deposited for RF power density ($P_D$) from 1.0 to 2.4 W·cm$^{-2}$. The diffraction pattern of the target is shown for comparison.

Ca/P ratio as a function of $P_D$ (Figure 1). This result suggests that the Ca-P-based phase incorporated in the sample presenting is CaO or a mixture of CaO and TCP.

A detailed analysis of the Ca2p$_{3/2}$ XPS line did not reveal significant modifications as the Ca/P ratio was varied. The binding energy and the full width at half-maximum values of the Ca2p$_{3/2}$ line have been measured to be $347.3 \pm 0.1$ and $2.5 \pm 0.1$ eV when increasing the Ca/P ratio from $1.51 \pm 0.02$ to $1.82 \pm 0.02$, respectively. These data are characteristic for HA.[42] Therefore, from XPS data, we did not observe any evidence for the formation of other bonds than the ones corresponding to HA. This observation is in apparent contradiction with the conclusion drawn from XRD results. Nevertheless, these data can merely be understood by considering that the binding energy of

CaO is $\approx 347.3$ eV,[43] and hence very close to the 347.5 eV corresponding to HA.[42] Overlapping of the two components in the Ca2p$_{3/2}$ spectra of sample containing additional Ca-based phases is therefore likely.

The measured elastic modulus values of the coatings as a function of the Ca/P ratio are shown in Figure 3. The elastic modulus increases from $131 \pm 11$ to $163 \pm 5$ GPa as the Ca/P ratio is increased from $1.51 \pm 0.02$ to $1.74 \pm 0.02$. A further increase in the Ca/P ratio to $1.82 \pm 0.02$ resulted in a decrease in the average elastic modulus of $\approx 15\%$.

As already discussed in the introduction, the mechanical properties of HA coatings depend on many parameters such as density, phase composition, crystallinity, and composition. Many studies on this subject are available in the literature but to the best of our knowledge, none of them are related to RF-sputtered HA films. For instance, Kweh et al. investigated the mechanical properties of plasma-sprayed HA coatings by Knoop and Vickers indentations.[44] Varying the particles size, spray distance, and annealing the deposited coatings at different temperatures, the authors have prepared HA coatings obtaining $E$ values ranging between 10 and 32 GPa. They attributed this large scattering to microstructural defects (thermal microcracks, voids, etc.) present in the coatings. In an other work on plasma-sprayed HA coatings, Wen et al. have shown by nanoindentation experiments that the coatings, made of crystalline and amorphous regions, which possess significantly different $E$ ($\approx 83$ vs. $\approx 128$ GPa for amorphous and crystalline compounds, respectively), showing that crystallinity plays also an important role in the mechanical properties of HA.[45] Mechanical properties of PLD-deposited HA coatings have also been investigated by Nelea et al. again by nanoindentation.[9] Studying the effect of ultraviolet (UV) irradiation assistance on the PLD process, the authors have measured an increase in $E$ values from $\approx 120$ to $\approx 180$ GPa when UV irradiation was employed. They attributed this phenomenon to a significant densification of the films due to higher excited species bombardment and, overall, to a partial transformation of HA into other Ca-P-based compounds such as TTCP, DCP, and CaO.

In the present work, the density of the deposited coatings has been evaluated by combining Tof-EERDA and thickness measurements (Figure 1). The data show that, the here-studied power density variation did not affect the density of the films significantly. The measured density is within $\approx 15\%$ of the bulk density value of HA (3.15 g·cm$^{-3}$).[22] Therefore, we assume that the observed evolution of the elastic properties is only due to the power density-induced changes in the composition and constitution. The origin of the relatively large standard deviation of the density data may be associated with the difficulty to precisely define the interface between the coating and the silicon wafer in the Tof-ERDA spectra and
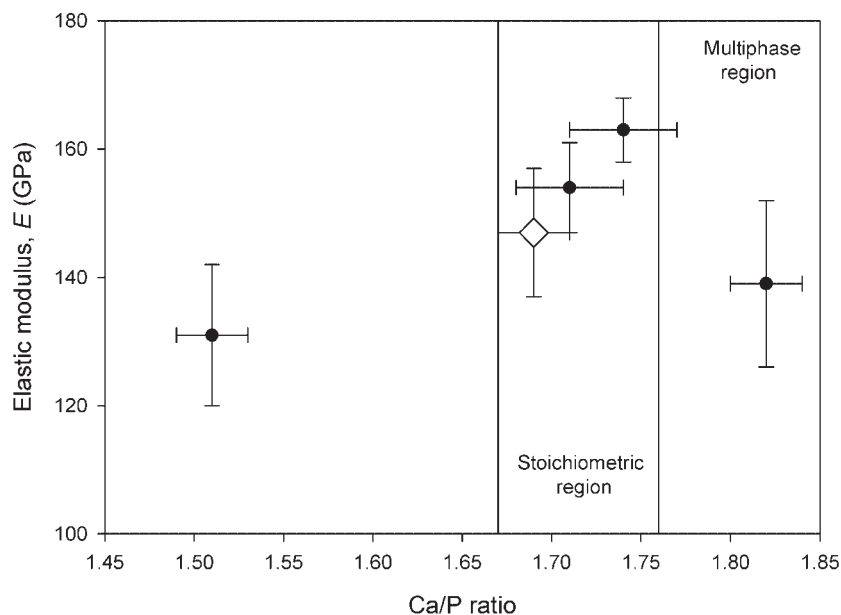
Influence of the Chemical Composition on the Phase Constitution and the Elastic Properties...

Plasma Processes
and Polymers



*Figure 3.* Evolution of the elastic modulus (*E*) and hardness (*H*) as a function of the Ca/P ratio value of the HA films. The unfilled diamond symbol corresponds to previously published data for pure, dense, and stoichiometric HA.[17] Acceptable HA stoichiometric Ca/P ratio region ranges between Ca/P = 1.67 and 1.74,[18] which is marked in the figure by vertical lines.

to the scattering of the thickness measurement due to thickness inhomogeneity and surface roughness.

The maximum elastic modulus value is obtained for a close to stoichiometric Ca/P ratio. The reduction of the elastic modulus from $154 \pm 5$ to $131 \pm 11$ GPa with the decrease in the Ca/P ratio value may be understood by the insertion of point defects in the HA cell, namely Ca vacancies in the structure to accommodate the deviation from the stoichiometric Ca/P ratio. A similar effect of vacancy insertion on the elastic properties of $Ti_4AlN_3$ has been published by Music et al.[46] The authors showed, using *ab initio* calculations, that N vacancy formation in $Ti_4AlN_3$ leads to a decrease in the bulk modulus by 10%. In order to support this assumption, we have estimated the bulk modulus (*B*), which is proportional to the elastic modulus, of a reduced stoichiometric HA unit cell (22 atoms) and of the same unit cell with one Ca vacancy (21 atoms) by *ab initio* calculations. These two configurations correspond to Ca/P ratio values of 1.67 (stoichiometric) and of 1.33, respectively. The value obtained for the stoichiometric cell deviates from the data calculated for a complete HA cell by $\approx$20%,[17] and by $\approx$14% from experimental data.[31] The removal of one Ca atom causes a decrease in *B* by $\approx$10% from 102 to 90 GPa. This result is consistent with the experimentally observed decrease in the elastic modulus. Hence, it is likely that the formation of Ca vacancies is responsible for the decrease discussed.

For Ca/P ratio value higher that the stoichiometric one, the elastic modulus decreases from $154 \pm 7$ to $139 \pm 13$ GPa. This phenomenon may be attributed to the appearance of other phases in the film which has been observed by XRD (Figure 2). Based on XRD results, the possible additional phases for this sample are CaO and TCP while the increase in Ca/P ratio for this sample suggests that CaO or a CaO + TCP mixture may be formed. Nevertheless, from the elastic modulus data, introduction of a phase presenting a lower elastic modulus than h-HA is expected and yet CaO has a higher elastic modulus than the one of h-HA. Actually, recent first-principle calculations have revealed that the independent elastic constants $C_{11}$, $C_{12}$, and $C_{44}$ for CaO are 215.13, 66.94, and 77.82 GPa, respectively.[47] Bulk (*B*), shear (*G*), and elastic (*E*) modulus can be obtained as follows:

$$B = \frac{1}{3}(C_{11} + 2C_{12}) \qquad (1)$$

$$G = \frac{1}{5}[(C_{11} - C_{12}) + 3C_{44}] \qquad (2)$$

$$E = \frac{9GB}{G + 3B} \qquad (3)$$

Using Equation (1)–(3), an elastic modulus of 180.2 GPa can be estimated within the isotropic approximation. Therefore, TCP for which *E* has been measured to be 115 GPa,[48] is likely to be present in this sample.

From the complete set of results (chemical composition, constitution, and mechanical properties), it is reasonable to assume that the sample with a Ca/P ratio value of $1.82 \pm 0.02$ prepared using the highest $P_D$ (2.4 $W \cdot cm^{-2}$) may actually be composed of a mixture of h-HA, CaO, and TCP.

## Conclusion

In this work, we have established the correlation between the target power density-induced changes in the chemical composition, the corresponding constitution, and elastic properties of RF magnetron-sputtered dense HA films. Varying the Ca/P ratio from $1.51 \pm 0.02$ to $1.82 \pm 0.02$, we have observed evidence suggesting the formation of CaO and $Ca_3(PO_4)_2$ for the highest Ca/P ratio value. The

maximum values of the elastic modulus are obtained for the stoichiometric compound. The reduction in elastic modulus observed when the Ca/P ratio is decreased may be understood by the insertion of Ca vacancies in the HA lattice, while the reduction of the average elastic modulus measured as the Ca/P ratio is increased to 1.82 is consistent with the constitution data. These results are significant for the application of HA films in load-bearing applications.

[1] ''CRC Handbook of Bioactive Calcium Phosphates'', K. de Groot, C. P. A. T. Klein, J. G. C. Wolke, J. M. A. de Bliek-Hogervorst, Eds., CRC Press, Boca Raton, FL, USA 1990.
[2] J. G. C. Wolke, J. P. C. M. van de Wearden, H. G. Schaeken, J. A. Jansen, *Biomaterials* **2003**, *24*, 2623.
[3] S. Koutsopoulos, *J. Biomed. Mater. Res.* **2002**, *62*, 600.
[4] K. de Groot, R. G. T. Geesink, C. P. A. T. Klein, P. Serekian, *J. Biomed. Mater. Res.* **1987**, *21*, 1375.
[5] R. J. Furlong, J. F. Osborn, *J. Bone Joint Surg.* **1991**, *73B*, 741.
[6] R. F. T. Geesink, *Clin. Orthop. Relat. Res.* **2002**, *395*, 53.
[7] H. Herman, *MRS Bull.* **1988**, *12*, 60.
[8] M. J. Filiaggi, N. A. Coombs, R. M. Pilliar, *J. Biomed. Mater. Res.* **1991**, *25*, 1211.
[9] V. Nelea, H. Pelletier, M. Iliescu, J. Werckmann, V. Craciun, I. N. Mihailescu, C. Ristocu, C. Chica, *J. Mater. Sci: Mater. Med.* **2002**, *13*, 1167.
[10] V. Nelea, C. Morosanu, M. Iliescu, I. N. Mihailescu, *Surf. Coat. Technol.* **2003**, *173*, 315.
[11] V. Nelea, C. Morosanu, M. Iliescu, I. N. Mihailescu, *Appl. Surf. Sci.* **2004**, *228*, 346.
[12] K. van Dijk, H. G. Schaeken, J. C. G. Wolke, C. H. M. Marée, F. H. P. M. Habraken, J. Verhoeven, J. A. Jansen, *J. Biomed. Mater. Res.* **1995**, *29*, 269.
[13] K. Ozeki, T. Yuhta, Y. Fukui, H. Aoki, *Surf. Coat. Technol.* **2002**, *160*, 54.
[14] K. A. Gross, C. C. Berndt, *J. Biomed. Mater. Res.* **1998**, *39*, 580.
[15] L. Cleries, E. Martinez, J. M. Fernandez-Pradas, G. Sardin, J. Esteve, J. L. Morenza, *Biomaterials* **2000**, *21*, 967.
[16] D. Liu, Q. Yang, T. Trozynski, *Biomaterials* **2002**, *23*, 691.
[17] R. Snyders, D. Music, D. Sigumonrong, B. Schelnberger, J. Jensen, J. M. Schneider, *Appl. Phys. Lett.* **2007**, *90*, 193902.
[18] Y. Yang, K. H. Kim, J. L. Ong, *Biomaterials* **2005**, *26*, 327.
[19] S. Xu, J. Long, L. Sim, C. H. Diong, K. Ostrikov, *Plasma Process. Polym.* **2005**, *2*, 373.
[20] H. Ozeki, H. Aoki, Y. Fukui, *J. Mater. Sci.* **2005**, *40*, 2837.
[21] B. Feddes, A. M. Vredenberg, M. Wehner, J. C. G. Wolke, J. A. Jansen, *Biomaterials* **2005**, *26*, 1645.
[22] ''Standard Reference Material Program'', National Institute of Standards and Technology, Gaitherburg, MD, USA 2003.
[23] K. van Dijk, H. G. Schaeken, J. C. G. Wolke, J. A. Jansen, *Biomaterials* **1996**, *17*, 405.
[24] ''Marvelous Biomaterial Apatite'', H. Aoki, Ed., Ishiyaku Publishers Inc., Tokyo, Japan 1999.
[25] K. van Dijk, J. Verhoeven, C. H. M. Marée, F. H. P. M. Habraken, J. A. Jansen, *Thin Solid Films* **1997**, *304*, 191.
[26] J. D. Long, S. Xu, J. W. Cai, N. Jiang, J. H. Lu, K. N. Ostrikov, C. H. Diaong, *Mater. Sci. Eng. C* **2002**, *20*, 175.
[27] J. R. Tesmer, M. Nastasi, ''Handbook of Modern Ion Beam Materials Analysis'', Material Research Society, Pittsburgh 1995.
[28] Y. Zhang, H. J. Whitlow, T. Winzell, I. F. Bubb, T. Sajavaara, K. Arstila, J. Keinonen, *Nucl. Instrum. Methods B* **1999**, *149*, 477.
[29] C. D. Wagner, L. E. Davis, M. V. Zeller, J. A. Taylor, R. H. Raymond, L. H. Gale, *Surf. Interface Anal.* **1981**, *3*, 211.
[30] W. C. Oliver, G. M. Pharr, *J. Mater. Res.* **1992**, *7*, 1564.
[31] S. J. Bull, *J. Vac. Sci. Technol. A* **2001**, *19*, 1404.
[32] D. E. Grenoble, J. L. Katz, K. L. Dunn, R. S. Gilmore, K. Linga Murty, *J. Biomed. Mater. Res.* **1972**, *6*, 221.
[33] P. Hohenberg, W. Kohn, *Phys. Rev.* **1964**, *136*, B864.
[34] G. Kresse, J. Hafner, *Phys. Rev. B* **1993**, *48*, 13115.
[35] G. Kresse, J. Hafner, *Phys. Rev. B* **1994**, *49*, 14251.
[36] D. Music, Z. Sun, J. M. Schneider, *Solid State Commun.* **2006**, *137*, 306.
[37] V. L. Moruzzi, J. F. Janak, K. Schwarz, *Phys. Rev.* **1988**, *B37*, 790.
[38] R. Snyders, J.-P. Dauchot, M. Hecq, *Plasma Process. Polym.* **2007**, *4*, 113.
[39] J. M. Schneider, A. Anders, B. Hjörvarsson, I. Petrov, K. Macák, U. Helmersson, J.-E. Sundgren, *Appl. Phys. Lett.* **1999**, *74*, 200.
[40] J. M. Schneider, B. Hjörvarsson, X. Wang, L. Hultman, *Appl. Phys. Lett.* **1999**, *75*, 3476.
[41] D. Music, H. Kölpin, A. Atiser, U. Kreissig, T. Bobek, B. Hadam, J. M. Schneider, *Mater. Res. Bull.* **2005**, *40*, 1345.
[42] S. Kaciulis, G. Mattogno, A. Napoli, E. Bemporad, F. Ferrari, A. Montenero, G. Gnappi, *J. Electron. Spectrosc.* **1998**, *95*, 61.
[43] H. Van Doveren, J. A. T. H. Verhoeven, *J. Electron. Spectrosc.* **1980**, *21*, 265.
[44] S. W. K. Kweh, K. A. Khor, P. Cheang, *Biomaterials* **2000**, *21*, 1223.
[45] J. Wen, Y. Leng, J. Chen, C. Zhang, *Biomaterials* **2000**, *21*, 1339.
[46] D. Music, R. Ahuja, J. M. Schneider, *Appl. Phys. Lett.* **2005**, *86*, 031911.
[47] Y. Deng, O.-H. Jia, X.-R. Chen, J. Zhu, *Physica B* **2007**, *392*, 229.
[48] M. Milosevski, J. Bossert, D. Milosevski, N. Gruevska, *Ceram. Int.* **1999**, *25*, 693.